Electronic Supplementary Material (ESI) for Dalton Transactions.

Supplementary Information for

Cooperative Spin-crossover Transition from Three-dimensional purely π-Stacking Interactions in a Neutral Heteroleptic Azobisphenolate Fe^{III} Complex with N_3O_3 Coordination Sphere

Suguru Murata,[a] Kazuyuki Takahashi,*[a] Tomoyuki Mochida,[a] Takahiro Sakurai,[b] Hitoshi Ohta,[c] Takashi Yamamoto[d] and Yasuaki Einaga[d]

[a]Department of Chemistry, Graduate School of Science, Kobe University, 1-1 Rokkodai-cho, Nada-ku, Kobe, Hyogo 657-8501, Japan. E-mail: ktaka@crystal.kobe-u.ac.jp

[b]Research Facility Centre for Science and Technology, Kobe University, 1-1 Rokkodai-cho, Nada-ku, Kobe, Hyogo 657-8501, Japan.

[c]Molecular Photoscience Research Centre, Kobe University, 1-1 Rokkodai-cho, Nada-ku, Kobe, Hyogo 657-8501, Japan.

[d]Department of Chemistry, Faculty of Science and Technology, Keio University, 3-14-1 Hiyoshi, Kohoku-ku, Yokohama, Kanagawa 223-8522, Japan

Contents

Experimental S2

Synthesis S2

Synthesis of [Fe(azp)(qsal)]·0.5MeOH (**1**) S2

Physical measurements S2

X-ray Crystal Structure Analyses S3

Data Collection, Structure Solution, and Structure Refinement S3

DFT Calculations S3

Table S1. Temperature variations of Mössbauer parameters for **1** S4

Fig. S1. DSC curve for **1**. S4

Table S2. The crystallographic data of **1** S5

Fig. S2. ORTEP drawing of 50% probability with atomic numbering scheme for **1**. S6

Table S3. Selected coordination bond lengths and distortion parameters. S6

Fig. S3. Top and side views of the intermolecular overlapping involving the π-stacking interactions at 90 and 273 K. S7

Table S4. The list of the calculated mean distances as the π-plane distances labelled in Table 1. S9

Table S5. Cartesian coordinates of the HS [Fe(azp)(qsal)] molecule. S10

Table S6. Cartesian coordinates of the LS [Fe(azp)(qsal)] molecule. S12

Fig. S4 Electronic absorption spectra simulated from the TD-DFT calculations for the [Fe(azp)(qsal)] molecule S14

References S15

Experimental

Synthesis. All reagents were obtained from commercial sources and used without further purification. Homoleptic SCO Fe^{III} complexes $[Fe(qsal)_2]Cl\cdot 1.5MeOH$ and $(TBA)[Fe(azp)_2]$ were synthesized according to the literature.[1,2]

Synthesis of [Fe(azp)(qsal)]·0.5MeOH (1). To a solution of $(TBA)[Fe(azp)_2]$ (60 mg, 0.083 mmol) in 80 mL of methanol was added a solution of $[Fe(qsal)_2]Cl\cdot 1.5MeOH$ (52 mg, 0.083 mmol) in 80 mL of methanol. To the resulting black solution was filtered and then stood at room temperature. After 1 day, **1** was obtained as black plate crystals (73.4 mg, 83.2%). Anal. Calcd for $C_{27.5}H_{21}FeN_4O_{3.5}$: C, 64.42; H, 3.98; N, 10.54%. Found: C, 64.43; H, 4.10; N, 10.51%.

Physical measurements. Variable temperature direct current magnetic susceptibilities of polycrystalline samples (ca. 15 mg) for **1** fold in an aluminium foil were measured on a Quantum Design MPMS-XL magnetometer under a field of 0.5 T and at a sweep speed of 2 K min^{-1} in the temperature range of 2-300 K. The sample magnetization data were obtained by the subtraction of background magnetization data for an aluminium foil from the measured data, and then the magnetic susceptibilities were corrected for diamagnetic contributions using Pascal constants.[3]

The photo effect on the magnetization was induced using a diode laser with 830 nm or 1060 nm diode head (Axcel Photonics) controlled by LDX-3545 precision current source (ILX Lightwave) and LDT-5525 temperature controller (ILX Lightwave). The light was guided by a quartz optical fibre into the sample chamber of the magnetometer. The grinded sample of **1** was dispersed in a hexane-acetone mixture by using an ultrasonic cleaning bath and then filtered using a hydrophobic PTFE type membrane filter (Advantec Toyo). The filtered sample powder on the membrane filter was fixed to the centre of a straw, whose end was connected with the end of an optical fibre placed in the sample chamber of the magnetometer. The measured data were corrected and scaled as compared with the magnetization data of a bulk sample.

The Mössbauer spectra were recorded on a constant acceleration spectrometer with a source of ^{57}Co/Rh in the transmission mode. The measurements at low temperature were performed with a closed-cycle helium refrigerator (Iwatani Co., Ltd.). The obtained Mössbauer spectra were fitted with symmetric Lorentzian doublets by the least squares fitting program (MossWinn).

The differential scanning calorimetry (DSC) analysis for **1** was performed with a TA instruments Q100 differential scanning calorimeter at a sweep rate of 10 K min^{-1} under a nitrogen atmosphere using aluminium hermetic pans with an empty pan as reference.

X-ray Crystal Structure Analyses

Data Collection, Structure Solution, and Structure Refinement. A crystal was mounted in a polyimide loop. A nitrogen gas flow temperature controller was used for the temperature variable measurements. All data were collected on a Bruker APEX II CCD area detector with monochromated Mo-Kα radiation generated by a Bruker Turbo X-ray Source coupled with Helios multilayer optics. All data collections and calculations were performed using the APEX2 crystallographic software package (Bruker AXS). The data were collected to a maximum 2θ value of 55.0º. A total of 720 oscillation images were collected. The APEX III program was used to determine the unit cell parameters and for data collection. Data were integrated by using SAINT. Numerical absorption correction was applied by using SADABS. The structures at all temperatures were solved by direct methods and refined by full-matrix least-squares methods based on F^2 by using the SHELXTL program. All non-hydrogen atoms were refined anisotropically. Hydrogen atoms were generated by calculation and refined using the riding model. The checkCIF for the CIFs of **1** at 90 and 273 K reported the ~~Alert level B and C due to unusually elongated ther~~mal ellipsoids in the azp ligand moiety. Since the single crystals of **1** had a heavily twinned nature, we are not sure that the Alert level B and C originate either from the twinning or from the orientational disorder in the azp ligand. Although we tried to refine the disordered models for the azp moiety at both temperatures, it was unsuccessful to refine the disordered model at 90 K. Thus, we refined the crystal structures without orientational disorder of the azp moiety. Additional details of the data collections and structural refinement parameters are provided in Table S2 and S3. ORTEP drawing of 50% probability with atomic numbering scheme for **1** is shown in Fig. S2. How to calculate the π-plane distances p, q, r, s labelled in Table 1 is shown in Table S4.

DFT Calculations. All theoretical calculations were performed using the Gaussian 09 program package.[4] All calculations of the compounds were carried out at the B3LYP functional[5,6] The Wachters-Hay basis set[7,8] for Fe atoms and the 6-31+G(d) basis set[9] for H, C, O, and N atoms were used. The atomic coordinates for the HS and LS states of the [Fe(azp)(qsal)] molecule were taken from the single crystal structural data of **1**. No imaginary frequencies were found in the optimized structures. Cartesian coordinates of the HS [Fe(azp)(qsal)] and LS [Fe(azp)(qsal)] molecules calculated by the B3LYP level of theory are summarized in Tables S4 and S5. The transition energies of all electron transitions of the HS [Fe(azp)(qsal)] and LS [Fe(azp)(qsal)] molecules were calculated by using the time-dependent DFT method[10] (TD-DFT) at the B3LYP level.

Table S1 Temperature variations of Mössbauer parameters for **1**.

Temperature / K	Spin state	*IS* [a] / mm s^{-1}	*QS* [b] / mm s^{-1}	Ratio
205	HS [c]	0.329(4)	0.888(6)	100%
	LS [d]	–	–	0%
170	HS	0.57(4)	1.28(7)	7.4%
	LS	0.036(2)	2.95(4)	92.6%
14.3	HS	–	–	0%
	LS	0.033(1)	2.958(3)	100%

[a] Isomer shift. [b] Quadrupole splitting. [c] High-spin. [d] Low-spin.

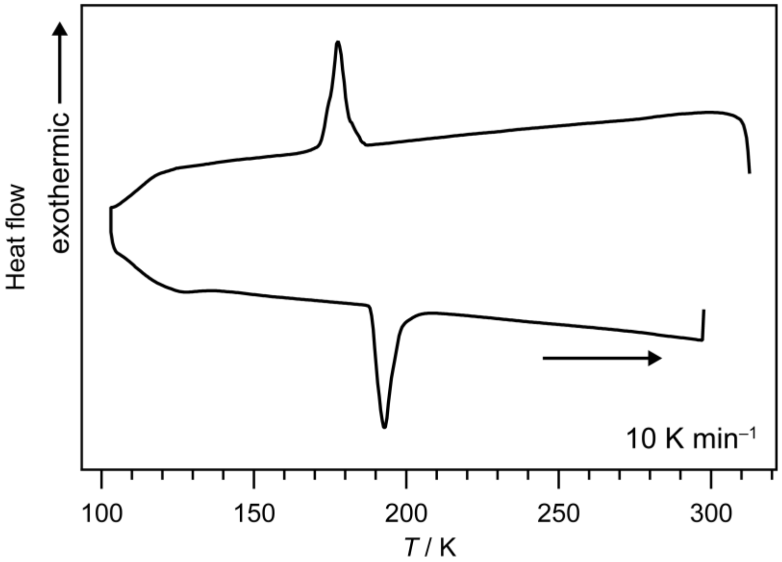

Fig. S1 DSC curve for **1** at a sweep rate of 10 K min^{-1}.

Table S2 The crystallographic data of **1**

	1	
Formula	$C_{28.5}H_{21}FeN_4O_{3.5}$	
Formula Weight	531.34	
Color	black	
Dimension / mm	0.07×0.07×0.02	
T / K	90	273
Crystal system	triclinic	triclinic
Space Group	P-1	P-1
a /Å	8.211(7)	8.3517(12)
b /Å	11.779(11)	11.4955(17)
c /Å	11.954(11)	12.5888(18)
α /°	95.645(13)	99.329(2)
β /°	100.928(12)	100.429(2)
γ /°	97.980(12)	95.311(2)
V /Å^3	1114.9(17)	1163.6(3)
Z	2	2
ρ_{calcd} / gcm^{-3}	1.583	1.516
μ (Mo-Kα)	0.722	0.691
$2\theta_{\mathrm{max}}$ /°	52.74	54.20
No. Reflections (R_{int})	5259 (0.0219)	6671 (0.0130)
No. Observations (I>2.00σ(I))	4318 (3399)	4981 (4040)
No. Variables	344	344
R1 (I>2.00σ(I))	0.0737	0.0564
R (all data)	0.0926	0.0707
wR2 (all data)	0.2032	0.1435
Residual electron density / eÅ^{-3}	2.032 –0.863	1.648 –1.207
Goodness of fit	1.047	1.045

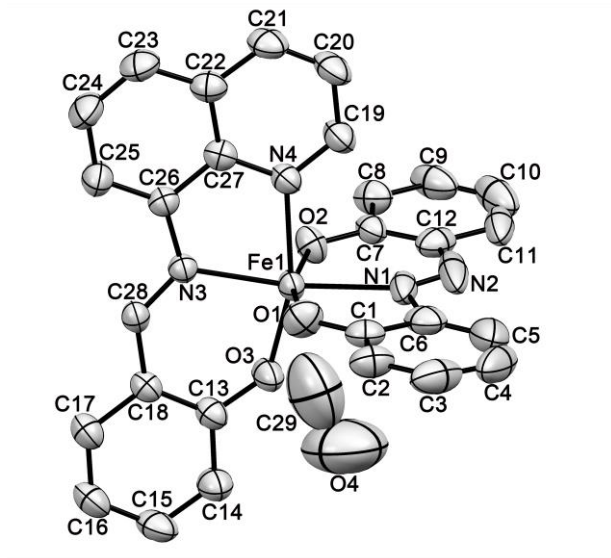

Fig. S2 ORTEP drawing of 50% probability with atomic numbering scheme for **1** at 273 K. Hydrogen atoms are omitted for clarity.

Table S3 Selected coordination bond lengths and distortion parameters for **1** and the related [Fe(azp)$_2$] and [Fe(qsal)$_2$] complexes.

	1		**(TMA)[Fe(azp)$_2$]**[2]		**[Fe(qsal)$_2$]·I$_3$**[11]	
T / K	90	273	90	273	50	293
Spin state	Low-spin	High-spin	Low-spin	High-spin	Low-spin	High-spin
Fe-O1/ Å	1.885(4)	1.954(3)	1.9233(15) ^{c}	1.975(2) ^{c}		
Fe-O2/ Å	1.871(4)	1.936(2)	1.8593(16) ^{c}	1.947(2) ^{c}	–	–
Fe-N1/ Å	1.908(5)	2.149(3)	1.9523(16) ^{c}	2.166(2) ^{c}	–	–
Fe-O3/ Å	1.882(3)	1.916(2)	–	–	1.887(6) ^{c}	1.914(7) ^{c}
Fe-N2/ Å	1.944(4)	2.122(3)	–	–	1.960(9) ^{c}	2.110(9) ^{c}
Fe-N3/ Å	1.975(4)	2.172(3)	–	–	1.986(7) ^{c}	2.130(6) ^{c}
Σ^{a} / °	40.84(16)	79.55(11)	47.95(5)	95.09(6)	39.0(3)	65.4(3)
Θ^{b} / °	52.49(14)	139.18(9)	62.51(13)	171.56(13)	57.4(2)	123.9(2)

[a] The sum of the absolute differences of bite angles from 90°. [b] The sum of the absolute differences of all the angles of triangle surfaces of a coordination octahedron from 60°. [c] The average lengths corresponding to the coordination bond lengths of **1**.

	90 K	273 K
p	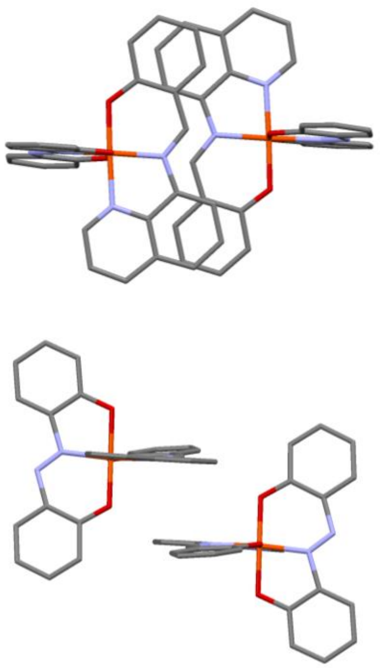	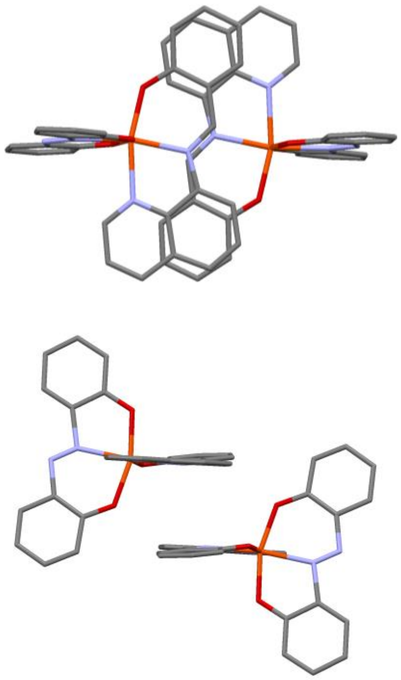
q	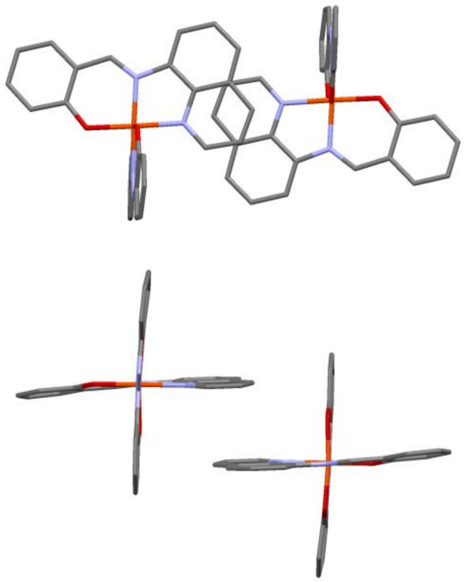	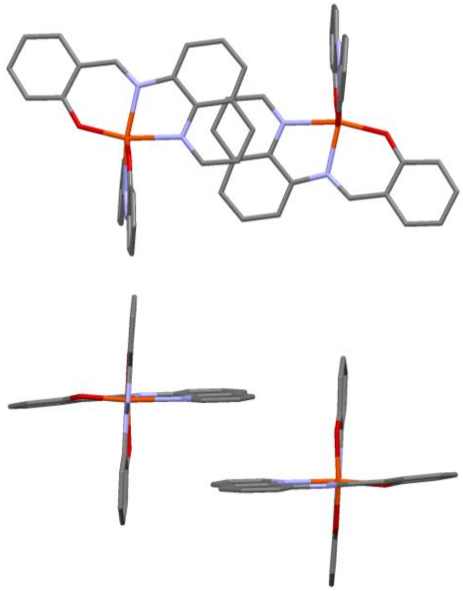

Fig. S3 Top and side views of the intermolecular overlapping involving the π-stacking interactions at 90 and 273 K. Hydrogen atoms are omitted for clarity.

	90 K	273 K
r	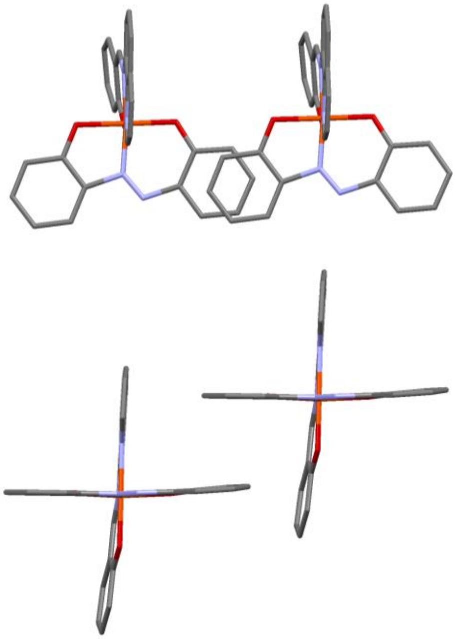	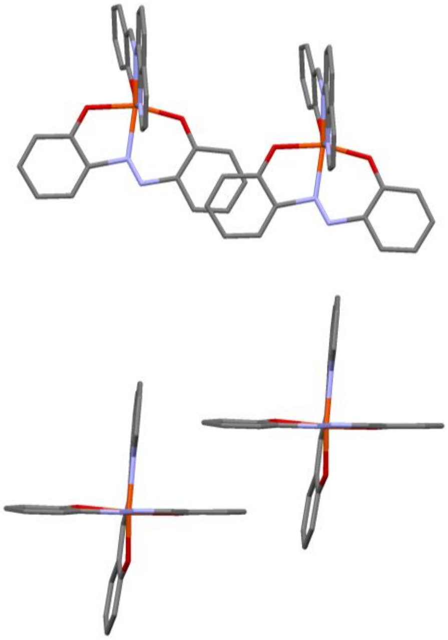
s	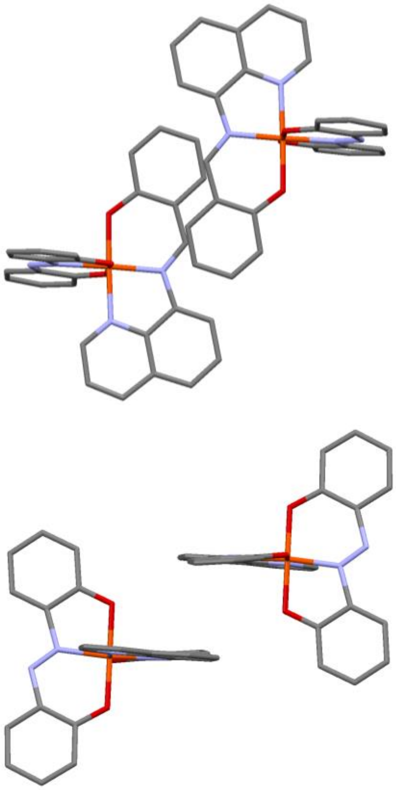	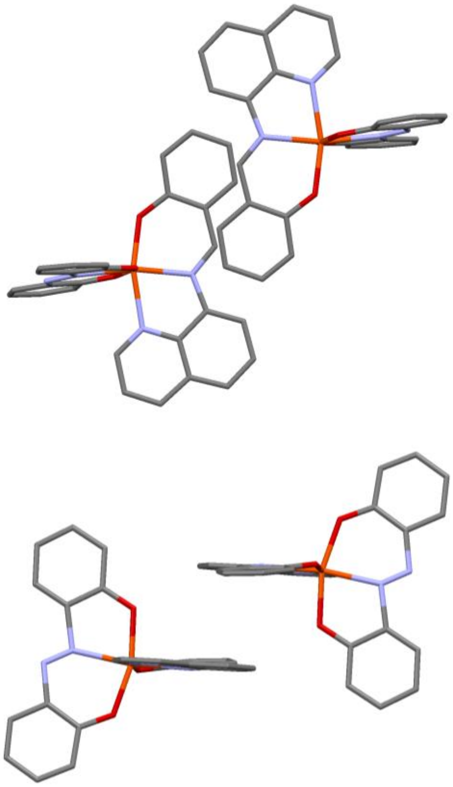

Fig. S3 (continue).

	90 K	273 K
t	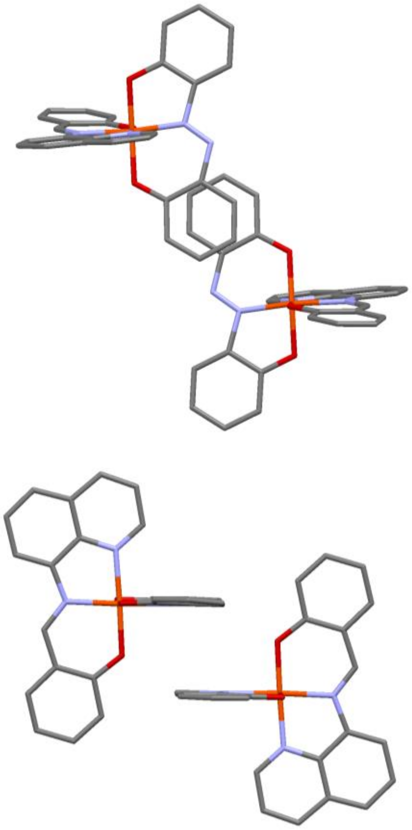	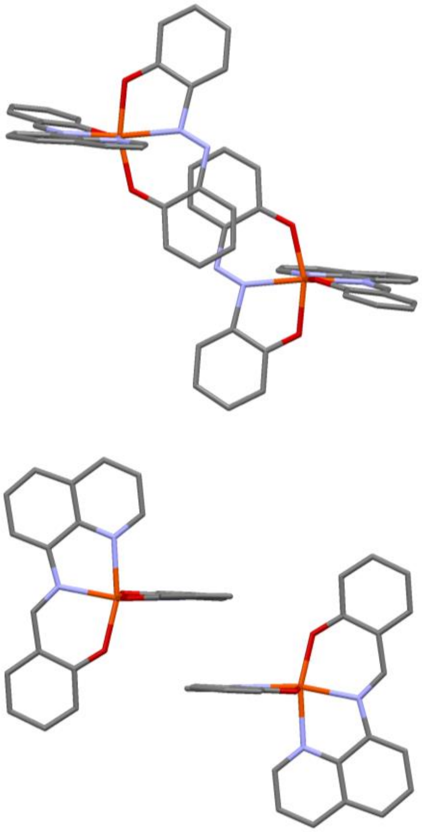

Fig. S3 (continue).

Table S4. The list of the calculated mean distances as the π-plane distances labelled in Table 1.

Labels	From	To
p	mean square plane (C13-C28,N3,N4)	mean square plane (C13-C28,N3,N4)$^{(a)}$
q	mean square plane (C19-C27,N4)	mean square plane (C19-C27,N4)$^{(b)}$
r	mean square plane (C1-C6)	atoms C8-C10$^{(c)}$
	mean square plane (C7-C12)	atoms C2-C4$^{(d)}$
s	mean square plane (C13-C18,C28)	mean square plane (C13-C18,C28)$^{(e)}$
t	mean square plane (C7-C12)	mean square plane (C7-C12)$^{(f)}$

Superscripts indicate symmetry operations. (a) (1-x,1-y,1-z) (b) (1-x,-y,1-z) (c) (1+x,y,z) (d) (-1+x,y,z) (e) (2-x,1-y,1-z) (f) (1-x,1-y,2-z)

Table S5. Cartesian coordinates of the HS [Fe(azp)(qsal)] molecule.

C	0.89579107	-1.14619309	2.41948318
C	0.85087706	-1.65020812	3.73840928
H	-0.12032801	-1.79780914	4.20202232
C	2.03099216	-1.94927615	4.41147234
H	1.98152215	-2.33705918	5.42656140
C	3.28690725	-1.76073013	3.80102629
H	4.19794232	-2.00276115	4.34131033
C	3.35624326	-1.26673009	2.50309119
H	4.30887233	-1.11503709	2.00583315
C	2.17155216	-0.95968707	1.81457614
C	2.02167415	0.67951305	-2.13320317
C	2.22951617	1.20362809	-3.43525326
H	1.35386810	1.54875312	-3.97766931
C	3.49545827	1.26216909	-3.99722730
H	3.61405628	1.66347013	-5.00127838
C	4.62744136	0.80912606	-3.28738125
H	5.61513143	0.85827207	-3.73620229
C	4.45894534	0.30288402	-2.01163715
H	5.30318340	-0.05397900	-1.42805511
C	3.17842724	0.22170802	-1.40840011
O	-0.19353801	-0.84963306	1.73810213
O	0.81423906	0.64700205	-1.63916513
N	2.08750516	-0.45243903	0.50509404
N	3.18311424	-0.29015502	-0.12671201
C	-1.41086211	-2.66022520	-1.01530608
C	-1.26468909	-4.03134031	-1.36422210
H	-0.26442402	-4.38373634	-1.59698112
C	-2.35504818	-4.88129337	-1.39103611
H	-2.20838717	-5.92665644	-1.65349312
C	-3.65506028	-4.41801134	-1.08183708
H	-4.50108034	-5.09818539	-1.10517809

C	-3.82895529	-3.08854924	-0.75490006
H	-4.82302937	-2.71096521	-0.52140304
C	-2.73522621	-2.18059217	-0.71718306
C	0.55663805	2.67708920	1.18283009
H	1.54226612	2.24230317	1.32593310
C	0.29959402	4.02002031	1.54098312
H	1.09253008	4.61905735	1.97736115
C	-0.95468907	4.54183535	1.31172210
H	-1.18265909	5.57550140	1.56123812
C	-1.96481215	3.72658928	0.73803306
C	-3.27628625	4.18526832	0.44497803
H	-3.54293227	5.21519040	0.66707805
C	-4.18693632	3.32670026	-0.13504801
H	-5.18313840	3.68117028	-0.38537103
C	-3.84893929	1.98390515	-0.42308003
H	-4.58618835	1.35306010	-0.90956607
C	-2.59088320	1.48146212	-0.11567801
C	-1.61874012	2.37544018	0.43806203
C	-3.01659423	-0.81409006	-0.41844203
H	-4.07365931	-0.59001304	-0.24147802
Fe	-0.01373700	-0.19692402	-0.10207601
N	-2.15199316	0.16529801	-0.33347703
N	-0.36531903	1.88893314	0.65707705
O	-0.36489503	-1.89042814	-0.99138207

Table S6. Cartesian coordinates of the LS [Fe(azp)(qsal)] molecule.

C	-0.24177202	-1.52866512	-2.34995118
C	-0.55924104	-2.01367415	-3.63914628
H	-1.16631809	-1.39366811	-4.29243633
C	-0.09432501	-3.26000125	-4.04266431
H	-0.34626903	-3.62500428	-5.03587038
C	0.69875505	-4.05873731	-3.19220124
H	1.05378708	-5.02816638	-3.53024227
C	1.02993508	-3.59931628	-1.92288315
H	1.64582812	-4.18567332	-1.24884409
C	0.55963504	-2.34402818	-1.50670611
C	1.37983611	-0.50065904	2.26867417
C	1.81081814	-0.08722701	3.55608627
H	1.41276611	0.85087706	3.93258130
C	2.70416721	-0.83992706	4.30176333
H	3.01284523	-0.48269704	5.28172840
C	3.21536425	-2.05734216	3.80636929
H	3.91548430	-2.64282920	4.39495834
C	2.81027021	-2.49178719	2.55762920
H	3.17764224	-3.42380826	2.13682017
C	1.90447515	-1.74204613	1.76604614
O	-0.66932905	-0.36507303	-1.90110815
O	0.51411304	0.25331602	1.63562013
N	0.82642906	-1.72994913	-0.26624602
N	1.59797312	-2.32353818	0.54870004
C	2.00220115	1.92069315	-0.95184107
C	3.34126226	2.19264417	-1.36140811
H	3.98522130	1.33772510	-1.54389512
C	3.79948029	3.48571427	-1.51006511
H	4.82926237	3.65338128	-1.81768614
C	2.95453923	4.59672435	-1.26862310
H	3.32849326	5.60898144	-1.38883011

C	1.65179913	4.36805433	-0.88369207
H	0.98328407	5.20740240	-0.69952005
C	1.13806409	3.04959824	-0.71689606
C	-2.17794917	-1.79204614	0.84174106
H	-1.42088111	-2.56782720	0.79427706
C	-3.49910027	-2.08835816	1.24709309
H	-3.75429929	-3.10762324	1.51829312
C	-4.43451734	-1.07827208	1.28135510
H	-5.46035942	-1.27833410	1.58112312
C	-4.05922931	0.24246902	0.92043607
C	-4.94828338	1.34881510	0.91318107
H	-5.98649543	1.20141309	1.19800409
C	-4.48677434	2.59369520	0.53455204
H	-5.16824540	3.43974426	0.51512204
C	-3.13827024	2.80039022	0.16403501
H	-2.83133522	3.79596629	-0.13832901
C	-2.23118917	1.74854113	0.17590201
C	-2.70409121	0.45237603	0.53926004
C	-0.22996602	2.91725522	-0.35095603
H	-0.77946906	3.85467029	-0.24206502
Fe	0.00390700	0.02632400	-0.16264701
N	-0.86282607	1.79185514	-0.14288101
N	-1.79949114	-0.57174705	0.49928304
O	1.64990712	0.67743205	-0.82462406

(a)

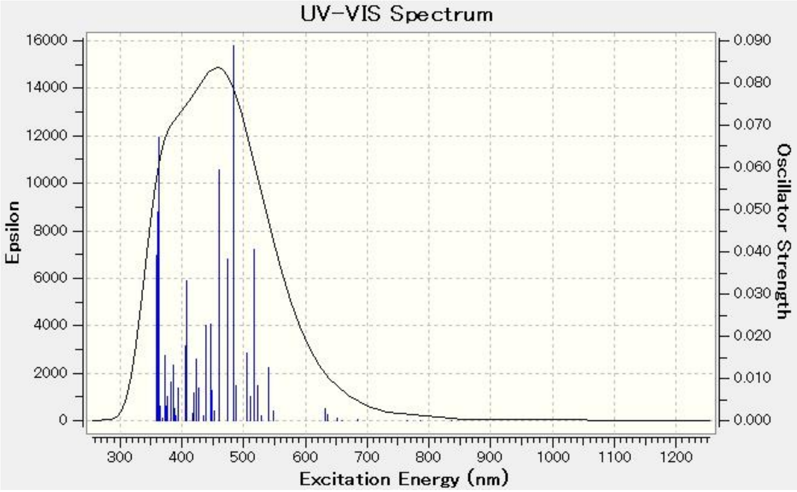

(b)

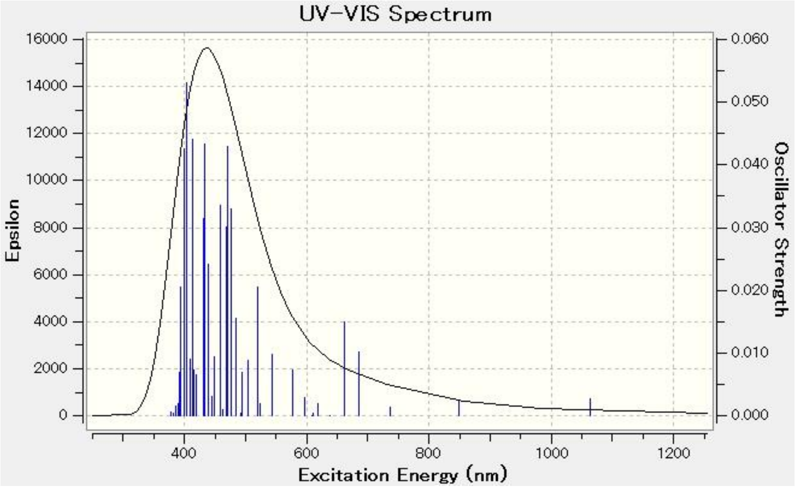

Fig. S4 Electronic absorption spectra simulated from the TD-DFT calculations for the [Fe(azp)(qsal)] molecule in the LS (a) and the HS (b) states.

References

[1] R. C. Dickinson, W. A. Baker and R. L. Collins, *J. Inorg. Nucl. Chem.*, 1977, **39**, 1531−1533.

[2] K. Takahashi, K. Kawamukai, M. Okai, T. Mochida, T. Sakurai, H. Ohta, T. Yamamoto, Y. Einaga, Y. Shiota and K. Yoshizawa, *Chem. Eur. J.*, 2016, **22**, 1253−1257

[3] E. König in *Landolt-Börnstein Neue Serie Gruppe II, Vol. 2* (Eds.: K.-H. Hellwege, A. M. Hellwege), Springer-Verlag, Berlin·Heidelberg·New York, 1966, pp. 1-16−18.

[4] Gaussian 09, Revision D.01, M. J. Frisch, G. W. Trucks, H. B. Schlegel, G. E. Scuseria, M. A. Robb, J. R. Cheeseman, G. Scalmani, V. Barone, B. Mennucci, G. A. Petersson, H. Nakatsuji, M. Caricato, X. Li, H. P. Hratchian, A. F. Izmaylov, J. Bloino, G. Zheng, J. L. Sonnenberg, M. Hada, M. Ehara, K. Toyota, R. Fukuda, J. Hasegawa, M. Ishida, T. Nakajima, Y. Honda, O. Kitao, H. Nakai, T. Vreven, J. A., Jr. Montgomery, J. E. Peralta, F. Ogliaro, M. Bearpark, J. J. Heyd, E. Brothers, K. N. Kudin, V. N. Staroverov, R. Kobayashi, J. Normand, K. Raghavachari, A. Rendell, J. C. Burant, S. S. Iyengar, J. Tomasi, M. Cossi, N. Rega, J. M. Millam, M. Klene, J. E. Knox, J. B. Cross, V. Bakken, C. Adamo, J. Jaramillo, R. Gomperts, R. E. Stratmann, O. Yazyev, A. J. Austin, R. Cammi, C. Pomelli, J. W. Ochterski, R. L. Martin, K. Morokuma, V. G. Zakrzewski, G. A. Voth, P. Salvador, J. J. Dannenberg, S. Dapprich, A. D. Daniels, Ö. Farkas, J. B. Foresman, J. V. Ortiz, J. Cioslowski and D. J. Fox, Gaussian, Inc., Wallingford CT, 2009.

[5] A. D. Becke, *J. Chem. Phys.*, 1993, **98**, 1372−1377.

[6] C. Lee, W. Yang and R. G. Parr, *Phys. Rev. B*, 1988, **37**, 785−789.

[7] A. J. H. Wachters, *J. Chem. Phys.*, 1970, **52**, 1033−1036.

[8] P. J. Hay, *J. Chem. Phys.*, 1977, **66**, 4377−4384.

[9] R. Ditchfield, W. J. Hehre and J. A. Pople, *J. Chem. Phys.*, 1971, **54** 724−728.

[10] M. E. Casida, C. Jamorski, K. C. Casida and D. R. Salahub, *J. Chem. Phys.*, 1998, **108**, 4439−4449.

[11] K. Takahashi, T. Sato, H. Mori, H. Tajima and O. Sato, *Physica B*, 2010, **405**, S65−S68.